Size effects in the magnetic behaviour of $TbAl_2$ milled alloys

2007 J. Phys.: Condens. Matter 19 186214

(http://iopscience.iop.org/0953-8984/19/18/186214)

IOP PUBLISHING JOURNAL OF PHYSICS: CONDENSED MATTER

J. Phys.: Condens. Matter **19** (2007) 186214 (15pp) doi:10.1088/0953-8984/19/18/186214

Size effects in the magnetic behaviour of $TbAl_2$ milled alloys

D P Rojas, L Fernández Barquín, J Rodríguez Fernández, J I Espeso and J C Gómez Sal

Departamento CITIMAC, Universidad de Cantabria, Santander 39005, Spain

E-mail: rojasd@unican.es

Received 25 October 2006, in final form 7 March 2007
Published 11 April 2007
Online at stacks.iop.org/JPhysCM/19/186214

Abstract

The study of the magnetic properties depending upon mechanical milling of the ferromagnetic polycrystalline $TbAl_2$ material is reported. Rietveld analysis of the x-ray diffraction data reveals a decrease in the grain size down to 14 nm and a -0.15% variation in the lattice parameter, after 300 h of milling time. Irreversibility in the zero field cooled–field cooled (ZFC–FC) dc susceptibility and clear peaks in the ac susceptibility between 5 and 300 K show that the long-range ferromagnetic structure is inhibited in favour of a disordered spin arrangement below 45 K. This glassy behaviour is also deduced from the variation of the irreversibility transition with the field ($H^{2/3}$) and frequency. The magnetization process of the bulk $TbAl_2$ is governed by domain-wall thermal activation processes. In contrast, in the milled samples, cluster-glass properties arise as a result of cooperative interactions due to the substitutional disorder. The interactions are also influenced by the nanograin structure of the milled alloys, showing a variation in coercivity with the grain size, below the crossover between the multi- and single-domain behaviours.

1. Introduction

The study of *heterogeneous magnetic structures* is a matter that attracts a vast research effort due to the rich phenomena related to the existence of competing interactions. These may lead to the promotion of magnetic disorder and, as a consequence, to the existence of a variety of magnetic ground states commonly associated with spin-glass or re-entrant spin-glass behaviours [1]. Frequently, heterogeneous structures can also display some degree of *magnetic clustering*, as occurs for instance in colossal magnetoresistance oxides [2], strongly correlated systems [3] or amorphous Fe–Zr alloys [4, 5], to cite a few examples. In addition, many heterogeneous structures are included in the field of *nanomagnetism* research, as they are formed by magnetic nanograins in a metallic or insulating matrix, giving rise to giant magnetoresistance, exchange-bias and single-domain magnetic properties [6–8]. It is then

obvious that the existing relationship between the magnetic disorder and the existence of magnetic clusters of different sizes depends on the sample, enhancing or masking the different magnetic interactions.

The influence of disorder on the magnetic properties of the system comprising cubic GdX_2 (where X = Al, Pt, Ir, Rh and Mg) Laves phase compounds has been studied recently [9–14]. The underlying interest is connected to our above statements; this is a ferromagnetic system that is very sensitive to disorder (caused by atomic substitutions or milling processes) and, hence, is suitable for observing what degree of disorder is necessary to break down the long-range ferromagnetism. In particular, it was observed that, upon milling, the value of the Curie temperature, (T_C), depends on the crystallographic change in the lattice parameter and the electronic character of the conduction electrons [11]. The ferromagnetic contribution disappears and a glassy magnetic behaviour emerges at lower temperatures. Zhou and Bakker also discussed the intrinsic nature of the emerging phase that appears for long grinding times, when the crystallite size becomes constant [9]. Additionally, other analyses have considered the role of grain boundaries in these alloys in relation to the random anisotropy effects [12, 14]. However, such a role remains relatively unexplored, although it presents some similarities to other three-dimensional (3D) transition-metal milled samples [15].

In some studies [10, 13], the ac susceptibility revealed a curious behaviour in which the influence of domain-wall relaxation was apparent. In these studies, no particular discussion was brought forward in relation to possible size effects in the milled samples, which is surprising considering that the decrease in particle size when using mechanical alloying processes is a very common result in other metallic or non-metallic systems [16]. The ac susceptibility (χ_{ac}) is convenient for the study of the magnetic behaviour of ferromagnetic materials with different magnetic phases and/or dynamic properties. In particular, the out-of-phase component gives useful information about the energy losses which occur during the domain-wall movement and domain magnetization rotation by the ac magnetic field h. For instance, the study of both the real and imaginary parts of the $\chi_{ac}(T)$ has revealed the dynamics of domain walls in RAl_2 (R = Dy and Er) compounds [17]. It is worth noticing that most of the ac susceptibility results, including those reported for the milled GdX_2 Laves phase compounds, are constrained to the in-phase component.

In the present work a study of the ball-milled cubic $TbAl_2$ Laves phase alloy has been undertaken. This compound crystallizes in the cubic $MgCu_2$ structure and orders ferromagnetically, as in other rare-earth RAl_2 Laves phase compounds, with $T_C = 105$ K [18]. The value of the coercivity and remanence due to the magnetocrystalline anisotropy is larger with respect to the Gd compounds, as suggested from the value of anisotropy constant reaching $K = 7 \times 10^6$ J m^{-3} [19]. Hence, in particular, we will explore the ac susceptibility data in more detail to establish a comparison between the magnetic properties of bulk and milled $TbAl_2$. This will enable us to understand the effect due to the introduction of disorder. In addition, a deep structural characterization is also presented to correlate such effects with the eventual presence of single-domain magnetic grains. Finally, given the implications of the variations of the anisotropy with a possible grained structure at the nanoscale, we will also focus on the variation of coercivity with grain size, which is a fingerprint of magnetic coupling/uncoupling processes among clusters/grains [20].

2. Experimental details

The starting alloy was prepared in an arc furnace from stoichiometric amounts of Tb (3N Alfa) and Al (5N, Alfa) metals. Then, a mass of 5 g of alloy was crushed and milled in a planetary high-energy ball system (Retsch PM 400/2) at a rotation speed of 200 rpm, using a container

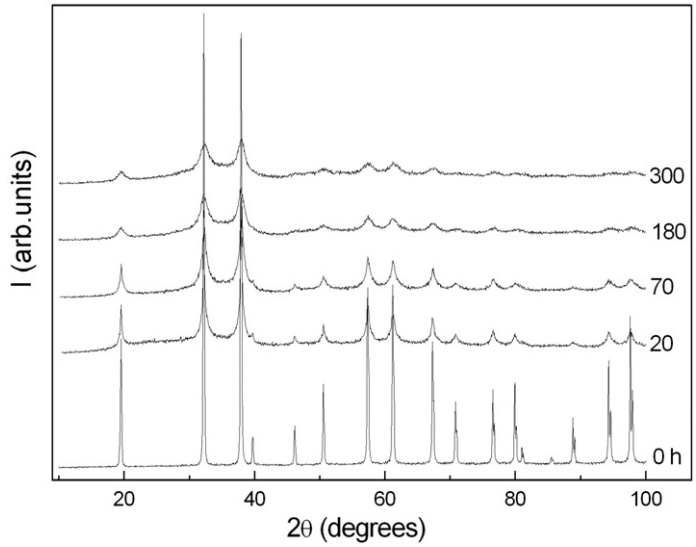

Figure 1. X-ray diffraction patterns for the as-cast (0 h) and milled samples. The grinding time (in hours) is indicated on the right. Patterns have been shifted up for clarity. The large width of the peaks in the samples milled for long times is evident.

and balls made of tungsten carbide. Small amounts of material were removed after 20, 70, 180 and 300 h of milling to perform measurements, always keeping the ball–sample weight ratio about 12. Handling and storage of the collected samples were carried out in a glove box under an argon atmosphere in order to prevent oxidation of the samples. The magnetic properties were collected in a Quantum Design PPMS in the temperature range 5–300 K and at frequencies of between 10 Hz and 10 kHz for χ_{AC} ($h = 1$ Oe) and magnetic fields of up to 9 T for the dc magnetization $M(H)$. Structural characterization was performed by collecting x-ray patterns in a Philips PW 1710 diffractometer, using Cu Kα radiation. The structural parameters were determined using a Rietveld powder profile programme [21] with silicon as a standard to correct for the instrumental broadening.

3. Results

3.1. Unmilled $TbAl_2$

The x-ray diffractogram of the unmilled sample (henceforth referred to as 0 h) is presented in figure 1. This starting compound was found to crystallize in the cubic $MgCu_2$-type of structure with a lattice parameter $a = 7.8619(6)$ Å, in agreement with that already reported [22]. The sample is single phase, as all reflections coming from the Laves phase $Fd\bar{3}m$ crystallographic space group were identified and no spurious phases were found.

Concerning the magnetic properties, the zero field cooled (ZFC) and field cooled (FC) curves of dc magnetic susceptibility (M/H) at a magnetic field of 500 Oe for a bulk sample is presented in figure 2. The existence of irreversibility is clearly evident. The temperature derivative of the FC magnetization is plotted in the inset. From this we can derive a precise value of the Curie temperature, $T_C = 105$ K.

Figure 3 displays both in-phase ($\chi'(T)$) and out-of-phase ($\chi''(T)$) components of the ac susceptibility obtained for the driving field of $h = 1$ Oe and for frequencies ranging from

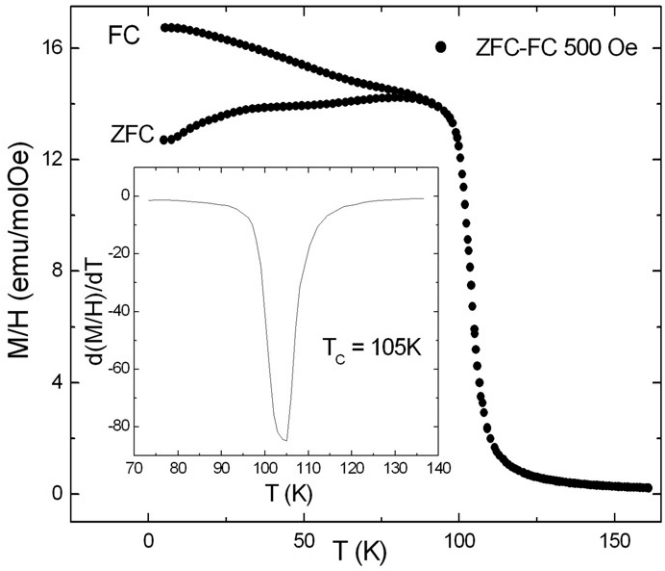

Figure 2. ZFC and FC curves of dc susceptibility at $H = 500$ Oe for the 0 h sample. The estimate of the transition temperature (T_C) is taken from the minimum of the first derivative, which is shown in the inset.

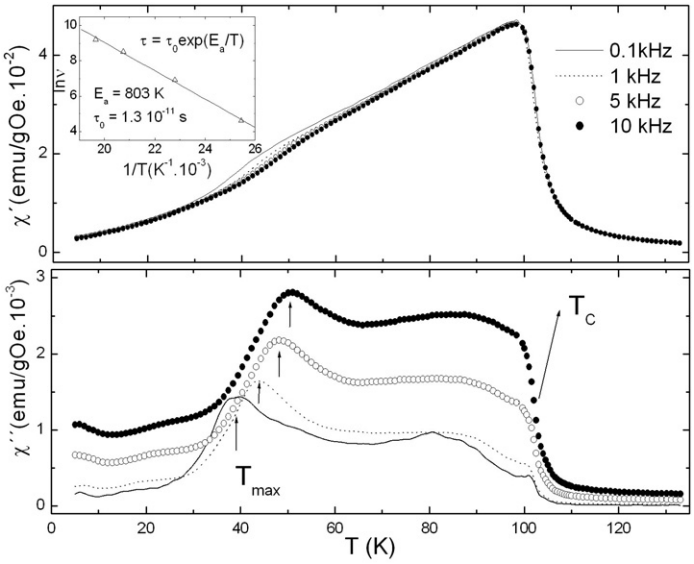

Figure 3. Thermal variation of the ac susceptibility, χ' and χ'', at several frequencies and $h = 1$ Oe for the $TbAl_2$ bulk sample. In $\chi''(T)$, the maximum around 40 K is associated, in magnetic bulk alloys, to domain-wall motion. The dynamics of this process results in a shift of the maxima, which are indicated by arrows (T_{max}). This effect can be described by a simple thermal activation process (Arrhenius law), as shown in the inset.

100 Hz to 10 kHz. In $\chi'(T)$, a frequency-independent transition shows a T_C value in agreement with the value estimated from the dc magnetization results. This confirms the existence of a

ferromagnetic–paramagnetic transition at T_C. A broad anomaly in $\chi'(T)$ between 30 and 60 K is smeared out with the increase in frequency. The curves depicted for the imaginary part $\chi''(T)$ reveal such a contribution in more detail. Three features can be observed: the ferromagnetic transition at $T_C = 105$ K; a broad anomaly around 80 K (more visible at the lowest frequency of 100 Hz); and a peak around 40 K which shifts to higher temperatures with the increase in frequency, as indicated by arrows. A similar behaviour has already been described in other cubic ferromagnetic rare-earth Laves phases such as $DyAl_2$ [17]. It is known that the imaginary component of the ac susceptibility is related to the absorption of energy by a ferromagnetic bulk material, which is caused by the domain-wall excitations. Across the domain wall, the spins change directions gradually due to the competition between magnetocrystalline and exchange energies. Thus, the clear rise in the peak of $\chi''(T)$ could be explained by dynamic domain-wall movements as a consequence of a thermal activation process. This process has been described well by a simple two-level model for the elementary excitations from the high to low energy levels [17, 23]. This approach leads to an Arrhenius relaxation law in which, if we plot the logarithm of the frequency of the ac magnetic field versus the inverse of the $\chi''(T)$ temperature maximum, the values for the relaxation time (τ_0) and the activation energy (E_a) can be estimated. Thus, the results of the ac susceptibility for the 0 h sample follows the above model and gives $\tau_0 = 1.3 \times 10^{-11}$ s and $E_a = 803$ K (69 meV). If compared with the results obtained for the ferromagnetic compounds $DyAl_2$ ($\tau_0 = 1.5 \times 10^{-8}$ s, $E_a = 40$ meV) [17] and Sm_2Fe_{17} ($\tau_0 = 1.7 \times 10^{-13}$ s, $E_a = 530$ meV) [23], then the value for the activation energy E_a is of the order of that in $DyAl_2$, but the relaxation time is between the values reported for $DyAl_2$ and Sm_2Fe_{17} and close to the attempt time of disordered magnets [24]. The differences in τ_0 and E_a are related to the magnetocrystalline anisotropy or softness (hardness) of the ferromagnetic material.

In the 0 h sample, as in any ferromagnetic material, the existence of an spontaneous magnetization and the formation of magnetic domains is expected. The thickness (δ) of the domain walls is determined by the competition between the magnetocrystalline anisotropy and exchange interactions. The width (δ) can be roughly estimated from the values of the exchange stiffness (A) and anisotropy constant (K). The parameter A can be calculated from the values of the Curie temperature, the lattice parameter a and the number of the nearest neighbours z, according to [25]:

$$A = \frac{3k_B T_C}{za}$$

where k_B is the Boltzmann constant. In consequence, for the 180° domain walls in cubic materials:

$$\delta = \pi\sqrt{\frac{A}{K}} = \sqrt{\frac{3k_B T_C}{zaK}} \tag{1}$$

and the domain-wall energy per unit area:

$$\gamma = 2K\delta. \tag{2}$$

In $TbAl_2$, $T_C = 105$ K, $a = 7.8619$ Å, $z = 4$ and, for the anisotropy constant, $K = 7 \times 10^6$ J m^{-3} [19]. Substituting these values in the expressions (1) and (2), values of $\delta = 1.4$ nm and $\gamma = 20$ mJ m^{-2} are obtained, below the values of $\delta = 40$ nm for Fe and 5 nm for $SmCo_5$ [25]. The higher values of the anisotropy constant in $SmCo_5$ and $TbAl_2$ lead to narrow walls in these materials when compared to Fe, which presents a lower magnetocrystalline anisotropy $K = 4.8 \times 10^4$ J m^{-3} and a higher value of $T_C = 1043$ K [25].

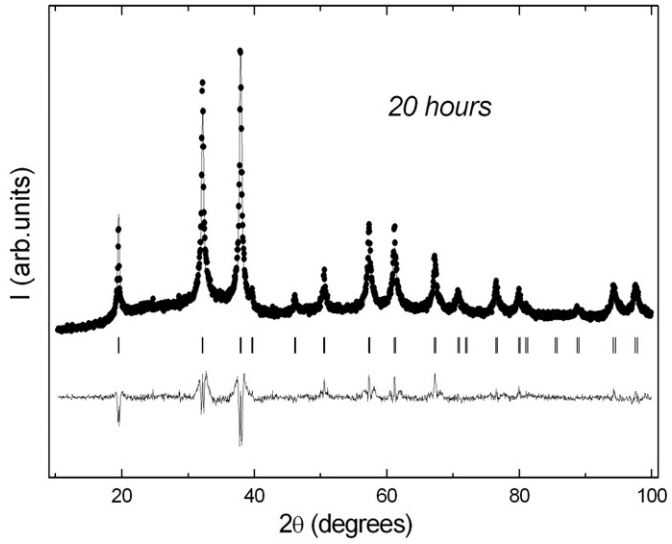

Figure 4. Rietveld refinement of the x-ray diffraction pattern for the 20 h milled sample. The experimental data are depicted by dots, the calculated refinement is represented by a continuous line, and the difference is the bottom line. The Bragg positions are indicated by vertical markers.

3.2. Milled $TbAl_2$ samples

X-ray diffraction patterns for the milled series are shown in figure 1. A progressive broadening and a reduction in the intensity of the peaks can be observed. This clearly indicates a decrease in the grain size [9–14], but it is also expected, although sometimes overlooked, that in metallic compounds a lattice strain is provoked by the milling. Although a Williamson–Hall analysis [26] can be carried out to extract both the grain size (D) and the strain (ε), it is most complete to perform a profile-fitting procedure of the diffraction peaks using the Rietveld method, which is not common in nanometric materials [27]. The parameterization of the Thompson–Cox–Hastings function establishes the variation of the profile peak width as a function of the scattering angle using Gaussian and Lorentzian peak shapes [28]. These peak contributions include two terms: one corresponding to the line broadening due to the size (proportional to $1/\cos\theta$) and another term, related to the strain broadening, depending on $\tan\theta$. The FULLPROF programme allows us to extract the crystallographic parameters and the values of D and ε using a peak profile analysis which also takes into account the instrumental broadening [21].

The results of the Rietveld refinement of the x-ray diffraction patterns are presented for the alloy milled for 20 h in figure 4, as an example. The refinement was carried out using the $Fd\bar{3}m$ space group, a Thompson–Cox–Hasting function for the peak profile, fixing the instrumental resolution function obtained for Si standard and with results for the Bragg errors $R_B \approx 15$, which are reasonable for x-ray diffraction pattern refinement. As a consequence, x-ray diffraction allows us to derive well-defined values for the grain size and strain, as was reported in other studies [29, 30], sampling a large volume in comparison with transmission electron microscopy images. The grain size decreases with milling time, as depicted in figure 5. This result will have consequences for evaluation of the magnetization and susceptibility curves. The smallest particle size, obtained for the 300 h milled sample, is about 14 nm. Further milling does not decrease this value. The general tendency is similar to that found

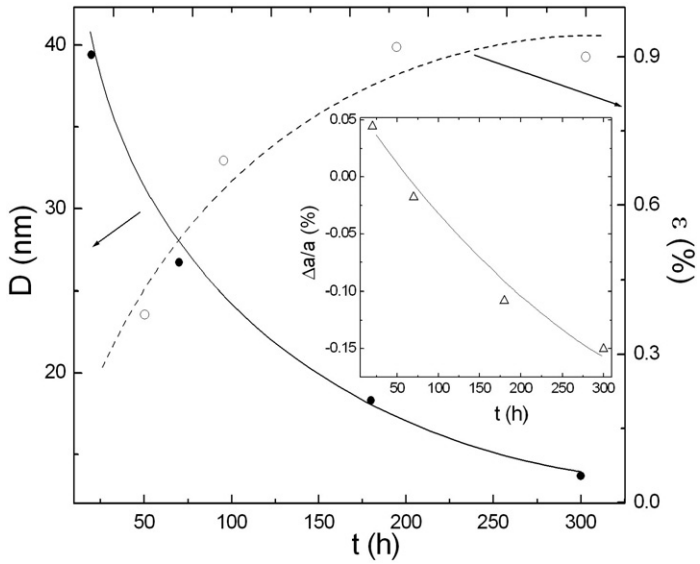

Figure 5. Particle diameter (D) (full symbols) and strain (ε) (open symbols) evolution as a function of the milling time. In the inset, the relative change in the lattice parameter upon milling is presented. The lines are guides for the eye. A diameter of $D < 20$ nm is reached for 300 h of milling time.

in other milled systems such as Fe–Cu–Ag [27] and Fe–Al [31], which are examples of heterogeneous magnetic systems. Figure 5 shows that the strain increases up to $\varepsilon \approx 1\%$, due to the introduction of disorder with grinding time, similar to what is observed in $GdAl_2$ [10] or Fe–Cu–Ag [32]. The strain also reaches a saturation for grinding times larger than 300 h. The inset of figure 5 shows the relative decrease in the lattice parameter $\Delta a/a = 0.15\%$ in the 300 h alloy with respect to the 0 h alloy, as was found in milled $GdAl_2$ compounds [10]. For this last series, the effect of the creation of site defects (the Al can substitute on the rare-earth sublattice) was suggested [10, 11], but the decrease in the size of the particles (to the nanometre scale) is another source for lattice variations, as some of the grains can present important lattice distortions.

Changes in the Curie temperature in the $GdAl_2$ milled series have been correlated with the variation of the lattice parameter and with disorder induced by mechanical milling [9–11]. These can be monitored from the ZFC and FC curves at $H = 50$ Oe, as shown in figure 6 for milled $TbAl_2$ alloys. The irreversibility of the ZFC and FC curves for a magnetic field of 50 Oe resembles the behaviour observed for re-entrant spin-glasses. Nonetheless, the FC curves do not saturate and the irreversibility is high compared to a canonical spin-glass. In this case, the system of particles seems to behave as a cluster-glass. A decrease in the T_C down to 102 K for the 20 h milled sample can be noticed in the M/H curve, and appears to be clearly defined in the derivative shown in the inset of figure 6. Regarding the 300 h milled sample, the T_C is barely observed in the M/H curves, but it is defined in the derivative shown in the inset, with $T_C = 98$ K. In the ZFC curve, a broad transition, confirmed in the inset, appears at 45 K. The dc susceptibility data (M/H) in the paramagnetic region, and for temperatures above 200 K, is described well by the Curie–Weiss law. The effective magnetic moment does not change significantly with $\mu_{\text{eff}} = 9.5 \pm 0.2\ \mu_B$ along the series, near to the theoretical value for a free Tb^{3+} ion of 9.72 μ_B. The positive sign of the paramagnetic Curie

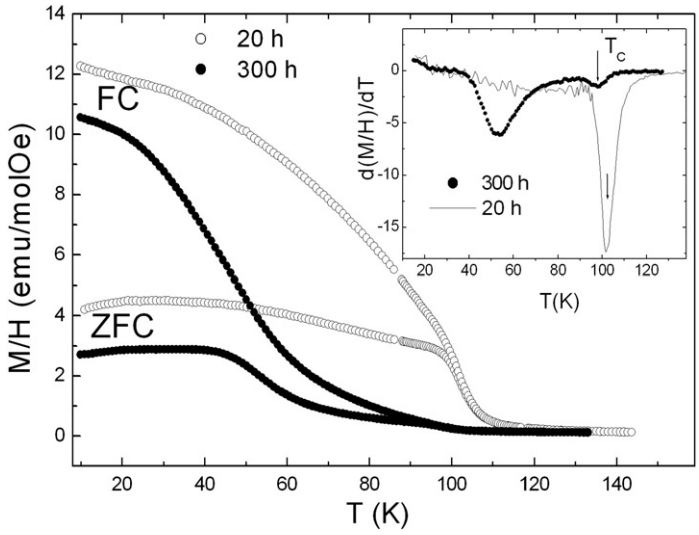

Figure 6. Temperature dependences of ZFC and FC susceptibility at $H = 50$ Oe for the 20 and 300 h milled samples. A large irreversibility is found in both cases. T_C is obtained from the derivative shown in the inset.

temperature (θ) indicates the presence of ferromagnetic correlations and a decrease from 106 K for the bulk to 7 K for the 300 h milled sample points towards a weakening of the exchange interactions [24]. The isothermal magnetization curves at $T = 5$ K as a function of the magnetic field reveal a decrease in the saturation magnetization (M_s) when increasing the grinding time, as observed in figure 7. This evolution suggests a canting of the magnetic moments at high magnetic fields, which can be due to the strong disorder and random anisotropy present in the alloy, similar to that observed in amorphous FeZr [4]. In addition, the grinding process results in the presence of nanometric grains, implying a canting of spins on the surface of the magnetic grains. Consequently, in this nanostructured $TbAl_2$, the domain-wall movement mechanism for multi-domain particles (observed in the bulk state) gives way to properties related to the nanoparticle state of the alloy.

The value of the coercivity (H_C) is strongly influenced by the magnetocrystalline anisotropy in the ferromagnetic state and by the grain size. The value of $H_C = 68$ Oe can be measured from the hysteresis loops, as shown for the 300 h milled alloy in the inset of figure 7. A decrease in H_C with grinding time is observed, and it can be correlated to a decrease in the grain size. This decrease on going to smaller magnetic grains is related to the crossover from multi-domain to single-domain magnetic grains [33]. The critical size for the appearance of single-domain particles can be estimated from the expressions for magnetostatic and domain-wall energies as follows [25]:

$$\frac{E_{ms}}{V} = \frac{\mu_0 M_s^2}{6}, \qquad \text{and} \qquad V = \tfrac{4}{3}\pi r^3$$

where μ_0 is the permeability of vacuum, M_s is the saturation magnetization, and r is the radius of the particle. Thus, the reduction in magnetostatic energy as a result of the division of the particle into two domains is $\Delta E_{ms} = E_{ms}/2V$. The wall energy for the particle with area πr^2 is $E_{wall} = \gamma \pi r^2$, with γ being the energy density per unit area. The reduction in energy by

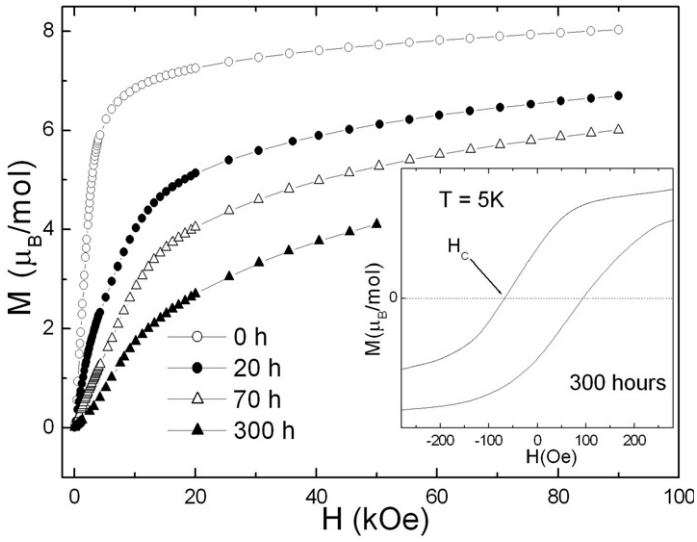

Figure 7. Magnetization curves as a function of the magnetic field for the 0, 20, 70 and 300 h milled samples at 5 K. The low-field region of the hysteresis loop for the 300 h milled alloy is shown in the inset. A value of $H_C \approx 70$ Oe is obtained for the coercivity.

splitting into two domains will be:

$$\Delta E = \gamma \pi r^2 - \pi \frac{\mu_0 M_s^2 r^3}{9}.$$

The condition for the critical size (r_c) is $\Delta E = 0$. Therefore, the critical radius of the single-domain particles is given by:

$$r_c = \frac{9\gamma}{\mu_0 M_s^2}.$$

From the $M(H)$ curve as a function of magnetic field at 5 K of the 0 h sample, a value of $M_s = 8.52\ \mu_B\ \text{mol}^{-1}$ is obtained. Taking $\rho = 5.82\ \text{g cm}^{-3}$ from the Rietveld refinement of the x-ray data, conversion to suitable units gives $M_s = 1.287 \times 10^6\ \text{A m}^{-1}$. Using the value for the domain-wall energy density estimated above, a critical radius for single-domain particles of $r_c = 85$ nm is calculated for the $TbAl_2$ alloy. Taking into account the average size obtained from the Rietveld refinements, $\langle D \rangle = 14$–39 nm, we expect single-domain particles for all milled samples.

Additional information about the evolution of the magnetic phases can be furnished by the temperature-dependence curves of $\chi'(T)$ and $\chi''(T)$, as shown in figure 8. The curves were obtained at $\nu = 10$ Hz and $h = 1$ Oe. The real component shows a smearing of the ferromagnetic transition and a peak around $T_f = 45$ K for the 300 h milled sample. The peak related to T_C shifts down to lower temperatures, with a decrease in particle size, whereas the tendency is not clearly observed for T_f. The nature of the peak at $T_f = 45$ K is further explored in the 300 h milled sample around the maxima. The $\chi_{ac}(T)$ results for this sample at different frequencies are presented in figure 9. It is particularly evident that the value of the maximum for $\chi'(T)$ (increases) and $\chi''(T)$ (decreases) with the increase of the frequency. This behaviour is standard in the magnetic relaxation of spin-clustered systems. Furthermore, the value for the relative shift per frequency decade, $\Delta T_f / T_f \Delta \log \nu = 0.0026(3)$, is similar to those reported for glassy magnets [24]. Quantitatively, the frequency dependence of the maximum can be

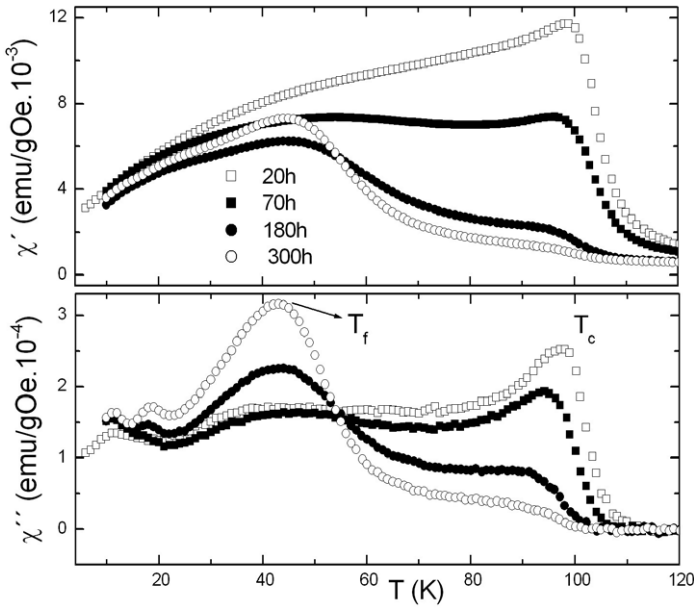

Figure 8. $\chi'(T)$ and $\chi''(T)$ for the series of milled samples at 10 Hz ($h = 1$ Oe). The ferromagnetic contribution decreases with an increase in milling time, evolving to a glassy arrangement below the peak at T_f.

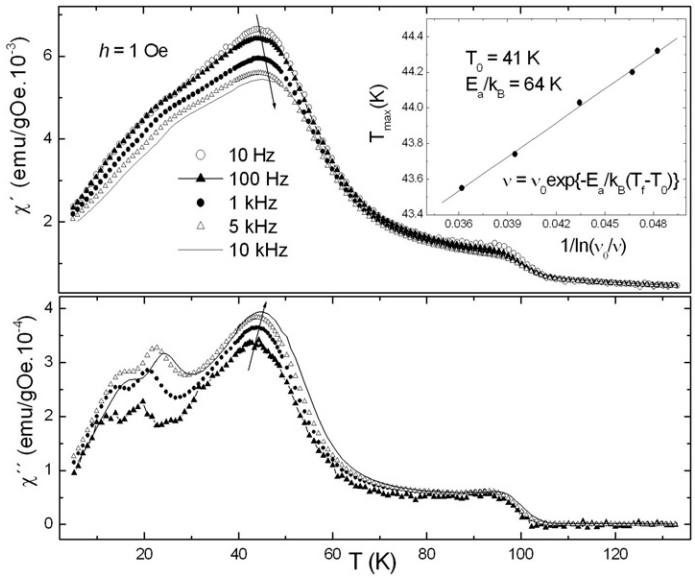

Figure 9. $\chi'(T)$ and $\chi''(T)$ at several frequencies for the 300 h milled alloy. In both cases, a shift of T_f with a variation in frequency is observed. The inset shows a fit to the Vogel–Fulcher law for spin-glasses.

reproduced by a phenomenological Vogel–Fulcher law using $\nu_0 = 10^{13}$ Hz, which is a value typical for spin-glass systems [24]. The result of the fitting yields a value of $T_0 = 41$ K for

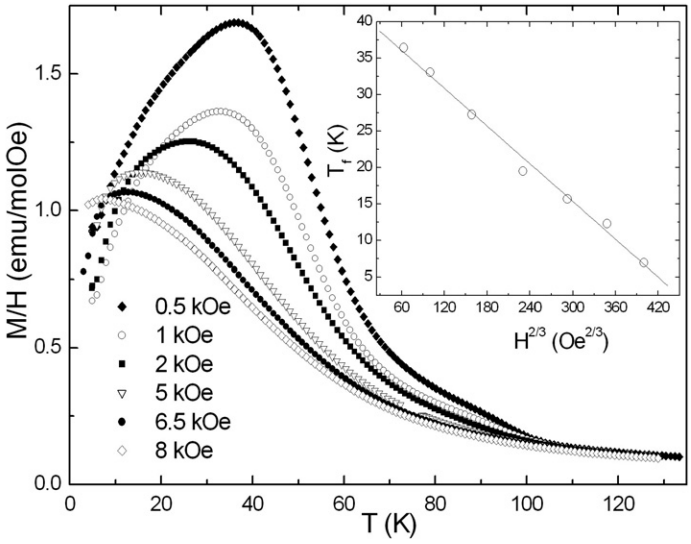

Figure 10. (a) Magnetic field dependence of the ZFC susceptibility as a function of temperature for the 300 h milled sample. In the inset, the magnetic field dependence of the ZFC susceptibility maxima (T_f) follows a $H^{2/3}$ law (Almeida–Thouless line), as found in spin-glasses.

the interaction temperature and $E_a/k_B = 64$ K for the activation energy, as shown in the inset of figure 9. Thus, a collective process of freezing of the spins rather than the domain-wall excitation is observed, as single-domain particles ($D < r_c$) are present in the milled $TbAl_2$ structure.

A further step in analysing the spin-glass transition can be performed by studying the field dependence of $M(T)$. In the ZFC curves for magnetic fields 1 kOe $< H <$ 8 kOe depicted in figure 10, a shift of T_f to lower temperatures with an increase in the dc magnetic field is observed. In the inset, the freezing temperature T_f as function of the magnetic field is plotted. The $T_f(H)$ follows a $H^{2/3}$ law (Almeida–Thouless line), which gives further proof for the freezing *(collective)*, as is commonly accepted [34].

4. Discussion

The results of the milling process in $TbAl_2$ polycrystalline alloy indicate, as seen in figure 1, a progressive decrease in the grain size and the absence of any new phase in the powder. The size reduction is commonly found in metallic and non-metallic systems, subjected to a mechanical milling process [16]. The trend for the crystalline size (D), and a concomitant increase in strain (ε) with milling time, has been evaluated using Rietveld refinement. As commented in the previous section, a minimum size of $D = 14$ nm and a maximum $\varepsilon \approx 1\%$ for the 300 h milled sample has been obtained. These values for size and strain are similar to other *cubic* rare-earth alloys or transition metals [10, 32]. In addition, the reduction in size is also connected to the variation in lattice parameters ($\Delta a/a$), in coincidence with previous studies on $GdAl_2$ [10].

The magnetic behaviour of $\chi_{ac}(T)$ for the bulk $TbAl_2$ alloy reflects the existence of a frequency-independent $T_C = 105$ K, with irreversible magnetic behaviour in the ZFC–FC curves. The ZFC curve is similar to that of $\chi'(\nu, T)$, although the lower ac driving field reflects more clearly the presence of strength of the anisotropy. This alloy is considered to be a ferromagnet [18] and the irreversibility stems from the competition between the

anisotropy and magnetization process as a result of the presence of magnetic domains [17, 23]. Indeed, the variations in $\chi''(\nu, T)$ are similar to domain-wall movements, as were already described in $DyAl_2$, and are in agreement with the understanding of an energy loss process due to its absorption by the domain walls [17, 23]. Nevertheless, it is striking to note that such behaviour is reminiscent of clustered magnetic (metallic) systems of a crystalline and amorphous nature [35, 36], in which a local anisotropy influences the magnetic behaviour. Hence, it might be plausible that, in this particular system, the size of the domains are reduced and are close to the nanometre scale, as is the case in magnetically disordered amorphous FeZr-based alloys [5]. In the following, we will discuss the variation produced by reducing the size of the particles.

In a fine-particle system the individual relaxation of the net magnetization of the magnetic grains gives rise to blocking/unblocking processes [7]. However, if the interparticle distances are small in those systems, strong interactions are expected among the particles. In our case, the structural study shows the existence of particles. These particles are below the single-domain size and, consequently, should show magnetic relaxation. However, the existence of grains in contact or with a narrow grain boundary modifies the relaxation phenomena, leading to a behaviour which is sometimes labelled as *superferromagnetism* [37]. This is very dependent on the nature of the grain boundary. If this grain boundary is paramagnetic, the magnetic atoms can become polarized and a ferromagnetic coupling can give rise to a great modification in the coercivity field [20, 38]. If the magnetic grain boundary is ferromagnetic, the connection between the grains is obvious, and the behaviour would match that of the bulk alloy. A qualitative picture of the magnetic structure of mechanically milled $GdAl_2$, composed of paramagnetic $GdAl_2$ grains, ferromagnetically aligned Gd-rich clusters in the grain boundaries and a Gd–Al grain boundary, has been proposed by Williams *et al* to explain the magnetic properties of this alloy [12].

By measuring the $M(H, T)$ and $\chi_{ac}(T)$, we can extract parameters leading to further insight. On the one hand, the $T_f(H)$ obtained from $M_{DC}(H, T)$ follows a $(H^{2/3})$ dependence of the ZFC maxima which is associated with glassy magnetic behaviour [34]. Recent reports on ferromagnetic nanograins with a large degree of interparticle (dipolar) interactions suggest that the variation should follow a $H^{1/2}$ dependence [39]; however, this is not the case in the $TbAl_2$ nanoparticle samples. On the other hand, the $\chi_{ac}(T)$ presents a dynamic behaviour in which, although the general shape is not far from that of bulk-$TbAl_2$, analysis of the $T_f(\nu)$ gives a low value for the relative shift per frequency decade of 0.0026(3) and can be fitted using the Vogel–Fulcher phenomenological law with $T_0 = 41$ K for the interaction temperature and $E_a/k_B = 64$ K for the activation energy in the 300 h-$TbAl_2$. This law is typically employed in magnetically disordered systems [24]. Thirdly, it is also worth mentioning here that the 70 and 180 h samples present a similar freezing temperature (approximately 45 K), whereas the size of grains is different (27 and 18 nm, respectively). This evidence seems to indicate that the freezing process is not strongly affected by the reduction in the particle size. Overall, these three experimental observations seem to suggest initially that the alloys present an intrinsic glassy behaviour. Such a behaviour has been interpreted as a result of the modification of the lattice parameters in the grain structure, giving rise to a quadrupole site defect mechanism where the Al atoms can substitute on the rare-earth sublattice, which has already been proposed for the GdX_2 milled series [10, 11]. This supplies the disorder and frustration within the magnetic grains, giving rise to a random anisotropy. Nevertheless, in other bulk intermetallic alloys of $CeNi_{1-x}Cu_x$, a magnetic clustering with nanometric spin correlations is found due to the substitution of Ni and Cu at random, presenting behaviours for $M(H, T)$ and $\chi_{ac}(T)$ similar to those reported here [3]. Accordingly, the clustering/grain effects cannot be ruled out in alloys in which the presence of nanometric grains is evidenced by x-ray diffraction data.

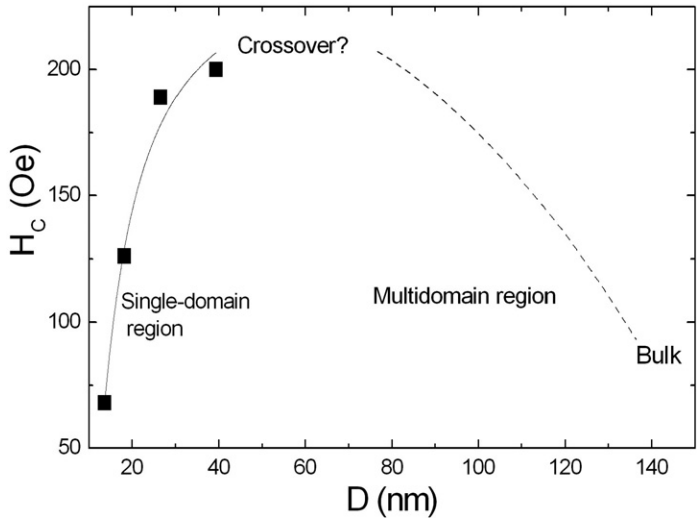

Figure 11. Size dependence of the coercivity (H_C). The milled alloys at 20, 70, 180 and 300 h appear within the single-domain region. The dashed line marks the tendency between the bulk and nanometre size alloys. A crossover between both behaviours is expected at about 60 nm. The solid line is the result of fitting to $H_C = g - h/D^{3/2}$.

A clear indication that the nanostructure is in an ingredient of the magnetic behaviour is provided by $H_C(D)$. The variation of the coercivity with the dimension of the particles can be divided into two regions corresponding to multi-domain and single magnetic domain. In the first region, starting from the larger size, a reduction in particle size leads to more pinning sites which result in an increase in H_C. Below the critical size, the particles become single-domain and, as the particle size decreases, H_C falls as $H_C = g - h/D^{3/2}$, where g and h are constants [33]. For the $TbAl_2$-milled samples, we obtained particles between 14 and 39 nm. These values are below the estimated critical radius of $r_c = 85$ nm, where the particles become single-domain. Consequently, the coercivity should decrease with the reduction in grain size, as is found here and shown in figure 11. The dependences found in our case agree with a decrease in H_C proportional to $D^{-3/2}$. This is striking, as it suggests that the grain boundary, which is probably formed by very distorted nanometric grains, is very weak from the magnetic standpoint, allowing a quasi-independent relaxation of the magnetic $TbAl_2$ grains. It also turns out that, if we compare the $H_C(D)$ with those of ferromagnetic grains surrounded by a paramagnetic grain boundary, as observed in many ultrasoft nanocrystalline alloys of the Fe–Nb–Cu–Si–B and Fe–Zr–Cu–B types [37], our results appear consistently away from their predictions, with a $H_C(D)$ decay proportional to D^6 due to a randomization of the anisotropy [20].

In view of the discussion just presented and the evident signs of collective freezing connected to a very disordered magnetic structure in the grains presented above, we propose that the magnetic structure of the nanostructured $TbAl_2$ is a collection of nanometric grains with sizes below the single-domain limit, in which the magnetic structure is highly disordered due to modification of the lattice parameter, favouring the existence of a random local anisotropy. This anisotropy is enough to promote freezing at 45 K, for all cases, but not enough to overcome the anisotropy associated with the nanometric grain structure. Given that the existence of nanoparticles in different matrices is usually related to *superparamagnetic* or *superferromagnetic* [37] behaviours, it is possible to consider that milled $TbAl_2$ is an example

of a *super spin-glass*, which has been suggested in other systems such as microcrystalline goethite [40], ferrite nanoparticles [41] and nanogranular $Al_{49}Fe_{30}Cu_{21}$ [42].

5. Conclusion

The influence of size effects on the magnetic properties of $TbAl_2$ alloy has been studied in mechanically milled alloys. Bearing in mind work already reported in the GdX_2 series, we have explored in more detail the results of the ac susceptibility as well as the changes in the coercivity upon milling through $M(H, T)$ measurements. Our Rietveld refinement at room temperature of the x-ray spectra indicates the formation of nanometric grains down to 14 nm in the 300 h alloy, with a strain reaching 1%. This reduction is clearly correlated to the variation of coercivity depending on grain size due to the presence of nanoparticles, which are situated below the crossover between the multi-and single-domain behaviours.

The dynamics of the magnetic relaxation, the field and the size dependence of T_f suggests the presence of an intrinsic disordered magnetic state inside the particles which leads to collective freezing, as occurs in *super spin-glasses*. The study of particles of sizes within the crossover region will lead to a deeper evaluation of how the local anisotropy in the grains is affected by the anisotropy effects that are typical of single-domain particles connected through a grain boundary.

Acknowledgments

This work was supported by the Direction of the Universities of the Ministry of Science and Education of Spain under contracts MAT 2003-06815, MAT 2005-04178-C04-02, SB2003-0102 and a Juan de la Cierva contract.

References

[1] O'Handley R C 1999 *Modern Magnetic Materials: Principles and Applications* (New York: Wiley) p 432
[2] Dagotto E, Hotta T and Moreo A 2001 *Phys. Rep.* **344** 1
[3] Marcano N, Espeso J I, Gómez Sal J C, Rodríguez Fernández J, Herrero-Albillos J and Bartolomé F 2005 *Phys. Rev.* B **71** 134401
[4] Ryan D H, Coey J M D, Batalla E, Altounian Z and Strom-Olsen J O 1987 *Phys. Rev.* B **35** 8630
[5] García Calderón R, Fernández Barquín L, Kaul S N, Gómez Sal J C, Gorria P, Pedersen J S and Heenan R K 2005 *Phys. Rev.* B **71** 134413
[6] Batlle X and Labarta A 2002 *J. Phys. D: Appl. Phys.* **35** R15
[7] Dormann J L, Fiorani D and Tronc E 1997 *Adv. Chem. Phys.* **98** 283
[8] Nogués J, Sort J, Langlais V, Skumryev V, Suriñach S, Muñoz J S and Baró M D 2005 *Phys. Rep.* **422** 65
[9] Zhou G F and Bakker H 1995 *Phys. Rev. Lett.* **74** 619
[10] Zhou G F and Bakker H 1995 *Phys. Rev.* B **52** 9437
[11] Modder I W, Bakker H and Zhou G F 1999 *Physica* B **262** 141
[12] Williams D S, Shand P M, Pekarek T M, Skomski R, Petkov V and Leslie-Pelecky D L 2003 *Phys. Rev.* B **68** 214404
[13] Morales M A, Williams D S, Shand P M, Stark C, Pekarek T M, Yue L P, Petkov V and Leslie-Pelecky D L 2004 *Phys. Rev.* B **70** 184407
[14] Shand P M, Stark C C, Williams D S, Morales M A, Pekarek T M and Leslie-Pelecky D L 2005 *J. Appl. Phys.* **97** 10J505
[15] Bonetti E, Del Bianco L, Fiorani D, Rinaldi D, Caciuffo R and Hernando A 1999 *Phys. Rev. Lett.* **83** 2829
[16] Suryanarayana C 2001 *Prog. Mater. Sci.* **46** 1
[17] Levin E M, Pecharsky V K and Gschneidner K A Jr 2001 *J. Appl. Phys.* **90** 6255
[18] Purwings H G, Houmann J G and Bak P 1973 *Phys. Rev. Lett.* **31** 1585
[19] Barbara B, Rossignol M F, Purwings H G and Walker E 1974 *Phys. Status Solidi* a **22** 553

[20] Herzer G 1989 *IEEE Trans. Magn.* **25** 3327
[21] Rodriguez-Carvajal J 1993 *Physica* B **192** 55 For recent versions and details consult the site: http://www.ill.fr/dif/Soft/fp
[22] Godet M, Walker E and Purwings H 1973 *J. Less-Common Met.* **30** 301
[23] Chen D X, Skumryev V and Coey J M D 1996 *Phys. Rev.* B **53** 15014
[24] Mydosh J A 1993 *Spin Glasses: an Experimental Introduction* (London: Taylor and Francis)
[25] Jiles D 1998 *Introduction to Magnetism and Magnetic Materials* (London: Chapman and Hall)
[26] Williamson G K and Hall W H 1953 *Acta Metallogr.* **1** 22
[27] Pankhurst Q A, Cohen N S and Odlyha M 1998 *J. Phys.: Condens. Matter* **10** 1665
[28] Snyder R L, Fiala J and Bunge H J 1999 *Defect and Microstructure Analysis by Diffraction* (New York: Oxford University Press)
[29] Fitzsimmons M R, Eastman J A, Müller-Stach M and Walner G 1991 *Phys. Rev.* B **44** 2452
[30] Guérault H and Greneche J-M 2000 *J. Phys.: Condens. Matter* **12** 4791
[31] Amils X, Nogues J, Surinach S, Baro M D, Munoz-Morris M A and Morris D G 2000 *Intermetallics* **8** 805
[32] Ucko D H, Pankhurst Q A, Fernandez Barquín L, Rodriguez Fernandez J and Cox S F J 2001 *Phys. Rev.* B **64** 104433
[33] Cullity B D 1972 *Introduction to Magnetic Materials* ed C Morris (Reading, MA: Addison-Wesley) p 383
[34] Almeida J R L D and Thouless D J 1978 *J. Phys. A: Math. Gen.* **11** 983
[35] Coey J M D 1978 *J. Appl. Phys.* **49** 1646
[36] Hansen P 1991 *Handbook of Magnetic Materials* vol 6, ed K H J Buschow (Amsterdam: Elsevier Science B V) p 289
[37] Kleemann W, Petracic O, Binek Ch, Kakazei G N, Pogorelov Yu G, Sousa J B, Cardoso S and Freitas P P 2001 *Phys. Rev.* B **63** 134423
[38] Herzer G 1998 *Handbook of Magnetic Materials* vol 10, ed K H J Buschow (Amsterdam: Elsevier Science B V) p 415
[39] Nunes W C, Socolovsky L M, Denardin J C, Cebollada F, Brandl A L and Knobel M 2005 *Phys. Rev.* B **72** 212413
[40] Mørup S, Madsen M B, Franck J, Villadsen J and Koch C J W 1983 *J. Magn. Magn. Mater.* **40** 163
[41] Kremenovic A, Antic B, Spasojevic V, Vucinic-Vasic M, Jaglicic Z, Pirnat J and Trontelj Z 2005 *J. Phys.: Condens. Matter* **17** 4285
[42] De Toro J A, López de la Torre M A, Riveiro J M, Bland J, Goff J P and Thomas M F 2001 *Phys. Rev.* B **64** 224421